

# Innovative Measurement Techniques and Applications of Aqueous Graphene-Based Conductive Paint

Rui Deng<sup>#</sup>, Fuze Shangguan<sup>#</sup>, Zhixuan Xia<sup>#</sup>, Shuoyi Liang<sup>#</sup>, Kuilong Wang<sup>\*</sup>

School of Physics, Hangzhou Normal University, Hangzhou, China, 311121

\* Corresponding Author Email: kuilongwang@hznu.edu.cn

<sup>#</sup>These authors contributed equally.

**Abstract.** Conductive paint, as a novel method to advance electronic product manufacturing technology in the coming decades, is gradually becoming a crucial element in inkjet printing and sensing and monitoring fields. In this study, we successfully prepared water-based conductive paint with nanographene as the base material through a simple solution mixing and dispersion-solidification process. Moreover, the prepared conductive paint can quickly solidify in the air and maintain its conductivity stability through multiple uses and measurements. We employed an improved Van der Pauw method in this research to measure the resistivity and sheet resistance of the conductive paint coated on a cellulose paper substrate, evaluating its conductivity. The results revealed an outstandingly low resistivity of  $(0.001404 \pm 0.000015) \Omega \cdot m$ . This remarkable conductivity highlights its enormous potential applications in areas such as sensors, flexible circuits, and wearable devices.

**Keywords:** Nanographene, Conductive Paint, Improved Van der Pauw Method, Perforated Material, Sheet Resistance.

## 1. Introduction

In the current context of technological advancement, conductive materials play a pivotal role in electronic engineering, materials science, and manufacturing, serving as the cornerstone in these fields. Over the past decade, significant progress has been made in the manufacturing technology of electronic devices, with the primary goals being miniaturization, portability, and efficiency[1]. Traditional silicon-based conductive materials struggle to meet the demands for characteristics such as miniaturization, ease of production, and cost-effectiveness, leading researchers to gradually shift their focus towards conductive ink. As a novel type of conductive material, conductive paint possesses advantages such as relatively simple manufacturing processes, low cost, strong scalability, and low environmental impact, making it highly attractive[2]. Many researchers believe that the integration of new conductive paint with efficient printing technologies could become a key method in manufacturing the next generation of electronic devices[4]. Therefore, leveraging its unique physical and chemical properties, conductive paint exhibits significant potential applications in areas such as sensors, flexible circuits, and wearable devices.

Due to the micrometer-level thickness of conductive paint when applied by inkjet printing or coating on a paper substrate [2], determining the volume resistivity is not a straightforward task. Therefore, we need to measure the sheet resistance. Sheet resistance represents the resistance of a two-dimensional, extended, and uniform square plane, commonly used in the semiconductor industry as part of thin-film electrical characterization [3]. When measuring the resistivity of thin films, non-contact methods (such as the infrequently used eddy current testing) or contact methods (most commonly the four-point probe technique) can be employed [4]. The Van der Pauw method is a variation of the four-point probe technique, primarily used for measuring the resistivity and Hall Effect coefficient of semiconductors [5]. It has also found widespread application in research; Dipankar Sahoo et al. used this method to measure resistivity and study the influence of adding MWCNTs on the resistivity of  $CH_3NH_3SnI_3$  [6]. Christian Golz et al. utilized this method to investigate the conductivity tensor of  $\beta$ -Ga $2O_3$  [7]. Masoomesh Ashoorirad et al. employed the Van der Pauw method to fabricate sensors for detecting moisture content in milk [8]. Simon Danninger et

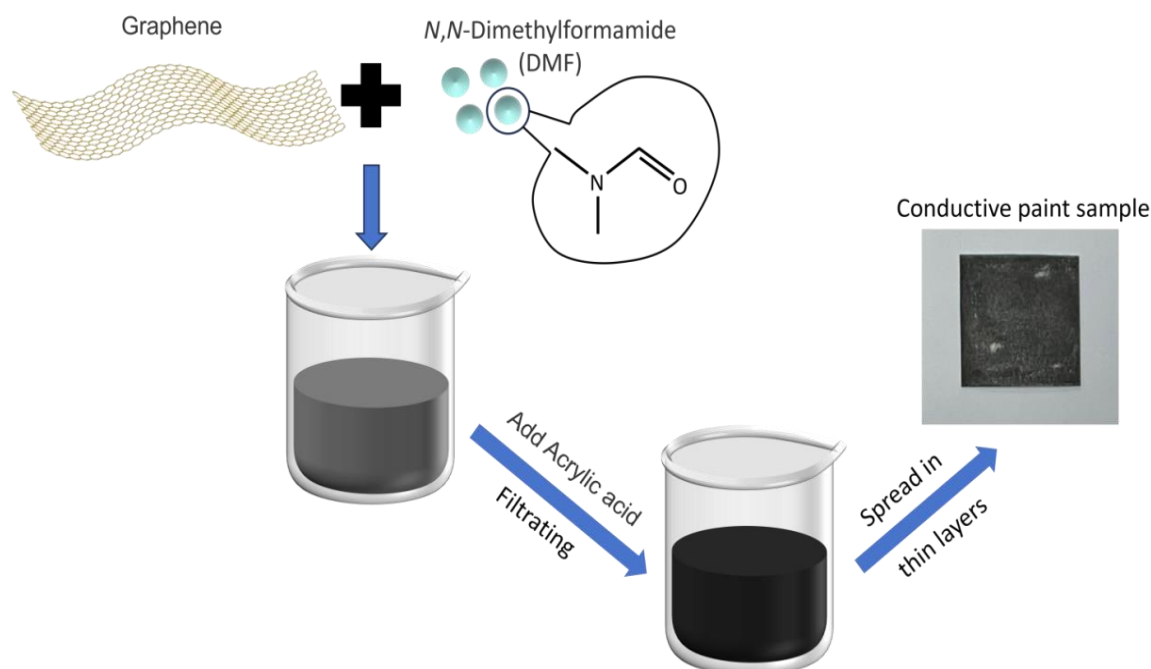
al. used the Van der Pauw method to measure the resistivity of DLC coatings deposited through a new process [8].

This study focuses on employing a relatively simple preparation method, specifically using a solution mixing and dispersion-solidification approach, to produce nanographene-based conductive paint. The Van der Pauw method is then utilized to assess the conductivity. During the process of using paper as the substrate for spray coating, the inherent viscosity of the conductive paint [9] leads to the presence of isolated holes of varying sizes on the sample surface, disrupting the fundamental conditions for Van der Pauw method measurements. Therefore, we developed an extended Van der Pauw method through simulation analysis, correcting the measurement errors caused by isolated holes. Experimental verification confirmed the accurate measurement of the resistivity of the conductive paint.

## 2. Preparation and Preliminary Characterization of Graphene-Based Conductive Paint

The current stage of research confirms the significant advantages of utilizing graphene to produce conductive paint. However, numerous formulations have achieved commercialization with high costs and potential exclusivity to specific applications [10]. Hence, exploring alternative simplified methods is advantageous for advancing research.

In this study, a method involving the dispersion of graphene with a dispersant followed by solution mixing was employed to formulate conductive paint, using DMF, acrylic acid, and water as supplementary materials. Initially, graphene powder was accurately weighed and dispersed in DMF, and after filtration, the dispersed graphene was uniformly mixed with acrylic acid. Finally, a small amount of distilled water was added, and the mixture was stirred thoroughly.



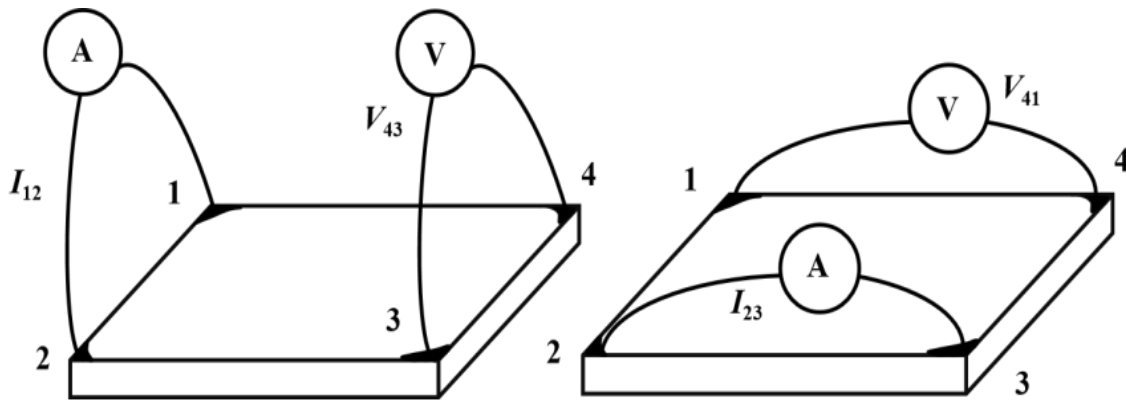
**Figure 1.** Preparation Process and Samples.

Figure 1 illustrates the preparation process and conductive paint samples, where the prepared conductive paint is sprayed onto a paper substrate to obtain thin film resistance samples. During the actual operation, it was observed that the inherent viscosity of the conductive paint resulted in the presence of isolated holes of varying sizes on the surface of the coated samples. The thickness of the samples meets the criteria for thin-film resistance, and the Van der Pauw method is employed for resistivity testing and conductivity assessment [4].

However, the isolated holes on the sample surface violate its essential measurement conditions. If a secondary coating is applied to fill the holes, there is a significant risk of uneven thickness on the sample surface, also violating the measurement conditions [5]. Therefore, it is necessary to make certain modifications to the Van der Pauw method to adapt it to the measurement of such conductive paint samples.

### 3. Method for Evaluation of Conductivity

Due to the theoretical impracticality of using the Van der Pauw method to assess the resistivity of conductive ink samples, we have modified and extended the Van der Pauw method based on constructing an equivalent electrical model and a mixed resistor grid. This modification allows for the measurement of the resistivity of the present conductive paint samples [5].



**Figure 2.** Schematic Diagram of Van der Pauw Method Electrode Measurements.

The Van der Pauw method reveals that, for a sample of arbitrary shape, four electrodes labeled 1, 2, 3, and 4 are fixed on its surface as shown in Figure 2. Electric current  $I_{12}$  is applied between two adjacent electrodes (e.g. 1 and 2), while the remaining two electrodes (3 and 4) measure the potential difference  $V_{34}$ . The resistance  $R_1$  is then calculated as  $R_1=V_{34}/I_{12}$ . Subsequently, the electrodes are swapped, and the other set (2 and 3) is used for passing electric current  $I_{23}$ , while the remaining two electrodes measure the potential difference  $V_{41}$ . The resistance  $R_2$  is then calculated as  $R_2=V_{41}/I_{23}$  and the thickness of the sample ( $d$ ) is measured. The resistivity can be computed using the transcendental equation known as the Van der Pauw equation [14].

$$e^{-\frac{\pi d R_1}{\rho}} + e^{-\frac{\pi d R_2}{\rho}} = 1 \tag{1}$$

The majority of studies contend that extending the Van der Pauw method necessitates modifications to the Van der Pauw equation. We define the Van der Pauw function  $v(R_1, R_2)$  to satisfy:

$$v(R_1, R_2) = e^{-\frac{\pi d R_1}{\rho}} + e^{-\frac{\pi d R_2}{\rho}} \tag{2}$$

The Van der Pauw function ( $v$ ) depends on the topological characteristics of the material, influenced collectively by  $R_1$  and  $R_2$ , referred to as the Van der Pauw resistances. When the sample surface is free of isolated holes,  $v=1$ , and the equation degenerates to the standard Van der Pauw equation. In the presence of holes,  $v \leq 1$  [12]. Thus, the geometric transition from a hole-free to a perforated surface is transformed into the problem of determining the Van der Pauw function  $v$ .

In Figure 3(a), a square conductive thin-film entity with side length  $L$  is considered to be composed of  $n \times n$  square thin-film resistance elements. It can be assumed that the current only passes through two directions perpendicular to the edges, the upward and downward, and left and right directions within each square thin-film resistance element with a side length of  $L/n$ . The remaining directions can be absorbed by projection in these two cases.

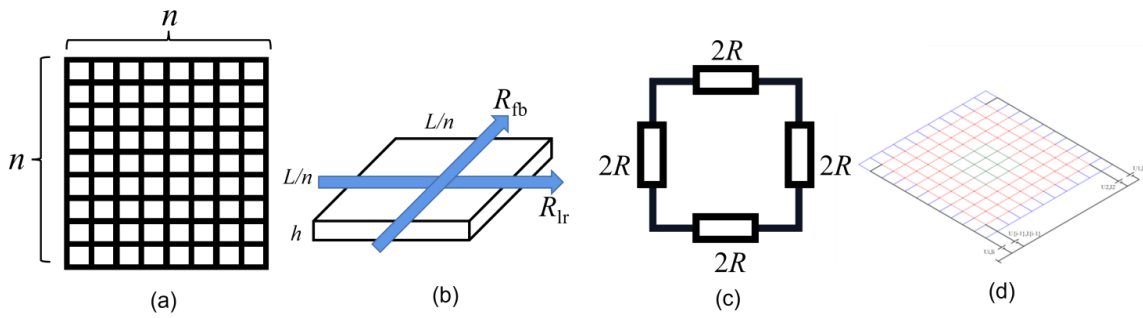


**Figure 3.** Construction diagram of the thin-film resistance grid.

(a) Thin-film resistances are divided into an  $n \times n$  grid. (b) Schematic diagrams of two different directional resistances. (c) Network of individual conductor grid resistance elements. (d) Result of constructing a mixed resistor grid for a perforated sample.

In the case of the entities square thin-layer resistor, if the current is defined to correspond to the resistance  $R_{lr}$  in the left-to-right direction and the resistance  $R_{fb}$  in the front-to-back direction, then  $R_{lr} = R_{fb} = \rho \frac{L/n}{(L/n)h} = \frac{\rho}{h}$ . Therefore, when  $\rho/h$  chosen as the unit resistance, the square thin-layer resistor element and the conductor grid resistor element in Figure 3(c) are electrically equivalent. Thus, as the grid density approaches infinity, the grid becomes the equivalent electrical model of the entity.

When constructing a mixed resistor grid for the entity using the equivalent electrical model, it is necessary to introduce resistance keys to describe the mixed resistor grid. The resistance key consists of three parts: resistance lines, used to build the conductive part of the sample, with each segment having a resistance of  $\rho/h$ ; insulation lines, used to create holes in the sample, with each segment having an infinite resistance; and superconductive lines, used to isolate external interference from the sample, with each segment having a resistance of 0.

Due to the linear relationship between the voltage  $V$  and current  $I$  in the structure of the grid, the transmission of the resistor grid can be described using a matrix. We use the current vector  $[I_1, I_2, \dots, I_m]^T$  to represent  $I$  and the voltage vector  $[V_1, V_2, \dots, V_m]^T$  to represent  $V$ , and it can be easily obtained that.

$$I = G \cdot V \quad (3)$$

Where  $G$  is an  $m \times m$  conductance matrix, reflecting the properties of the resistor grid, uniquely determined by the topological structure of the resistor grid.

Due to the correspondence between the construction of the mixed resistor grid and the transformation of the conductance matrix, the following rules (4) exist:

$$\begin{cases} G'_{ij} = G_{ij} - \frac{G_{i\alpha} G_{\alpha j} R}{1 + G_{\alpha\alpha} R} & i, j = 1, 2, \dots, m \\ G''_{ij} = G'_{ij} + \frac{(\delta_{\alpha j} - \delta_{\beta j})(\delta_{\alpha i} - \delta_{\beta i})}{R'} & i, j = 1, 2, \dots, m \end{cases} \quad (4)$$

Therefore, a uniquely determined conductance matrix can be obtained from the mixed resistor grid [13].

By solving the system of equations with the conductance matrix  $G$ , the corresponding current and voltage matrices for the resistor grid can be calculated. Subsequently, the coefficients  $v$  of the extended Van der Pauw method can be determined. It can be proven that when the grid density exceeds a threshold, the computation results must converge, ensuring the determination of the coefficients  $v$  in the extended Van der Pauw method.

To accurately represent the characteristics of holes in the sample, we use the size and position of the holes for characterization. Define the hole area ratio  $S = \text{hole area}/\text{total sample area}$ , hole offset  $B = \sqrt{\frac{B_x^2 + B_y^2}{2}}$ , and construct the conductance matrix for samples with different hole area ratios and hole offsets using a computer. Calculate the corresponding discrete values of the Van der Pauw function ( $v$ ). By fitting, it is possible to compute a bivariate function concerning the hole area ratio ( $S$ ) and hole offset ( $B$ ) as shown in Figure 4.

$$v(B, S) = e^{C_3 B - C_1 S^{C_2}} \tag{5}$$

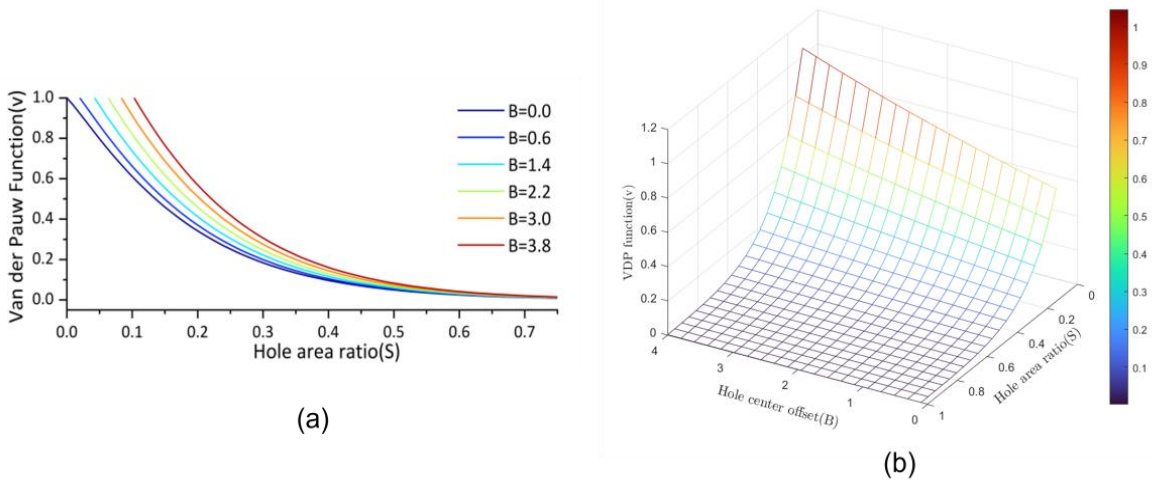


**Figure 4.** Fitting results of discrete values computed by the computer: Relationship between the Van der Pauw function and hole area ratio and offset.

#### 4. Experiment results and discussions

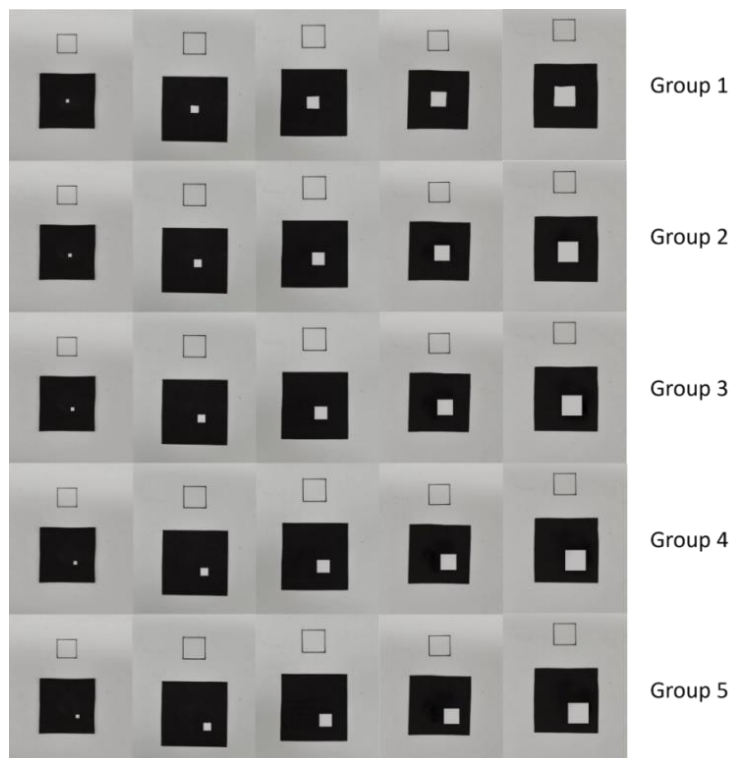


**Figure 5.** 25 sample slices with varying hole sizes and offsets.

To validate the correctness of this measurement method, we conducted a validation experiment using prepared conductive paint. The conductive paint was applied to a Dowling paper substrate, and the thickness of the sample slices was measured using a micrometer, yielding a thickness of 50  $\mu\text{m}$ . Professional laboratory assessment determined its sheet resistance to be 28 Ohms, corresponding to an electrical resistivity of  $1.4 \times 10^{-3}$  Ohm·m.

As shown in Figure 5, 25 test samples with different pore sizes and offsets were created using the conductive paint and sequentially labeled 1 to 25. The offsets and area ratios were measured, as depicted in Figure 6. Horizontal and vertical comparisons were conducted for both hole area ratio  $S$  (yellow columns) and hole offset  $B$  (blue-purple columns), leading to the following distinct conclusions:

- (1) The pore area ratio  $S$  of the same group increased sequentially from 0%, as follows: 0.411%, 1.421%, 3.612%, 6.691%, and 10.075%.
- (2) The offsets for Group 1, Group 2, Group 3, Group 4, and Group 6 were 0.0248 cm, 0.1984 cm, 0.4078 cm, 0.5984 cm, and 0.7974 cm, respectively.

The calculated Van der Pauw function is  $v(B, S) = \exp(0.1342B - 6.5397S^{1.1225})$ .

After calculating the Van der Pauw function values using equation (5) and subsequently substituting them into equation (1) for resistivity calculation, the results are illustrated in Figure 7 and Figure 8.

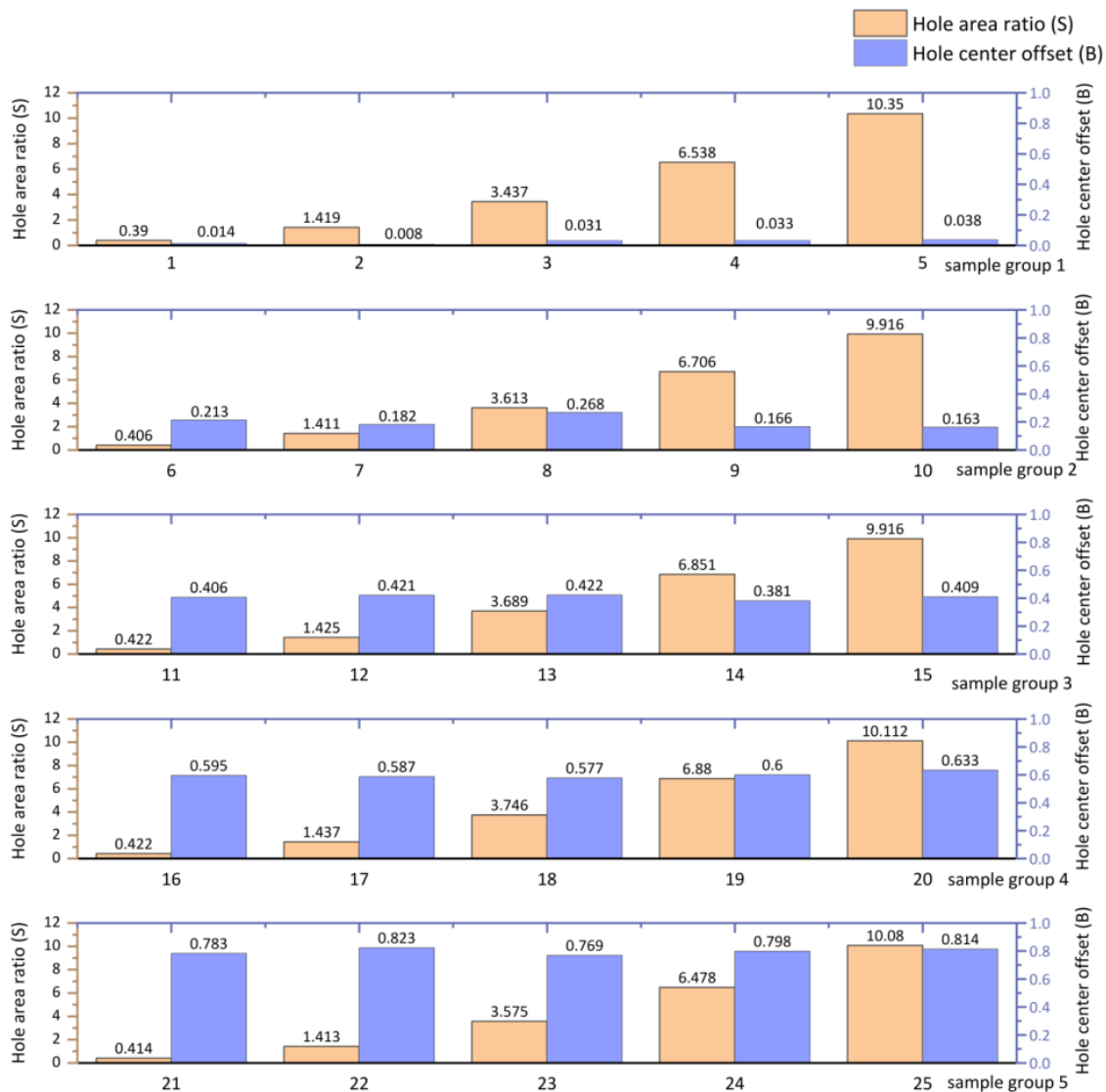


**Figure 6.** Assessment results of hole area ratio and offset for the sample slices.

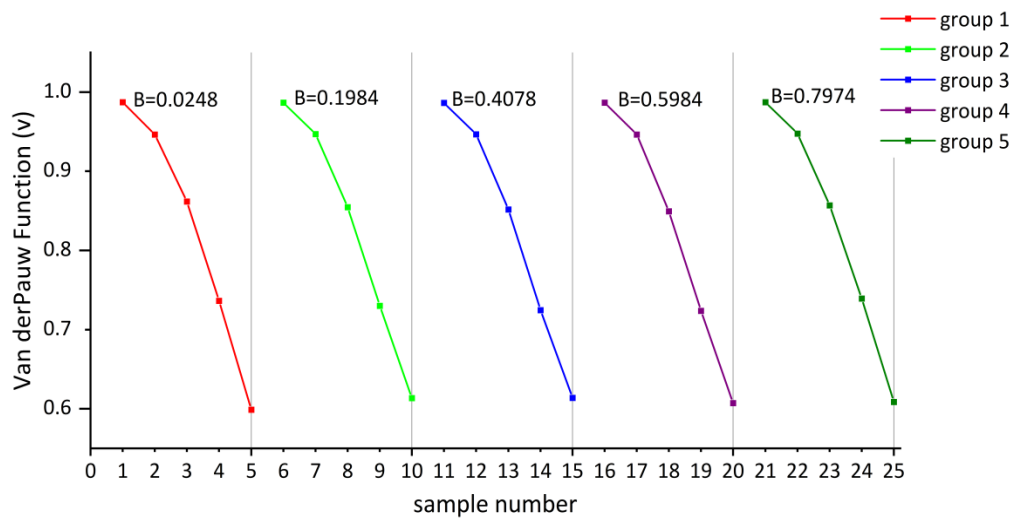


**Figure 7.** Calculated results of the Van der Pauw function for each sample slice.

As depicted in Figure 8, the resistivity measurement results for these 25 sample slices, obtained using the improved Van der Pauw method, are 0.001404 Ohm·m. Calculations based on the percentage error formula  $E_r = \frac{\rho_{msr} - \rho_{std}}{\rho_{std}} \times 100\%$  and the uncertainty formula  $U = \sqrt{U_a^2 + U_b^2}$  indicate a measurement percentage error of 0.65% and an uncertainty of 0.000015 Ohm·m.

Therefore, the comprehensive validation of the measurement results for the samples is  $(0.001404 \pm 0.000015)$  Ohm·m. This experimental outcome not only strongly supports the accurate measurement of the resistivity of the self-prepared conductive paint using the improved Van der Pauw method but also reflects the consistent conductivity stability of the prepared conductive paint throughout multiple uses and measurements.

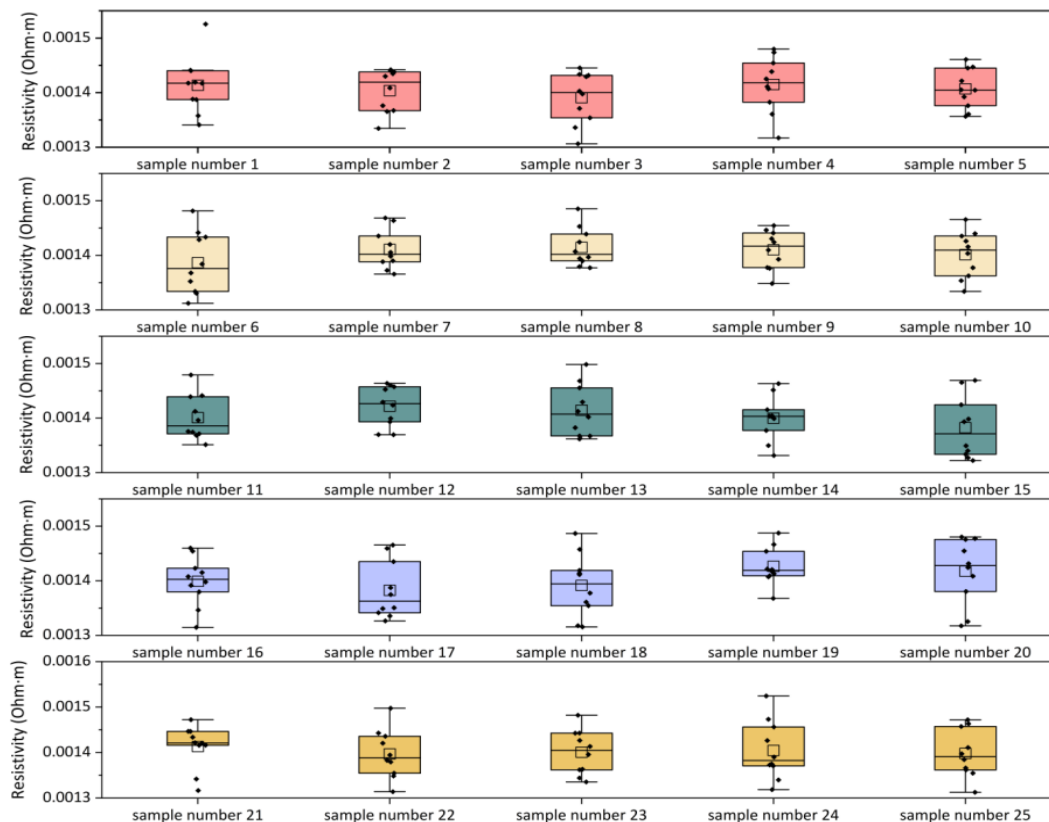


**Figure 8.** Results of the Van der Pauw function values and resistivity.

## 5. Conclusions

This study employed a straightforward solution mixing and dispersion-coagulation process to prepare water-based conductive paint with nano-graphene as the base material. To accurately assess the conductivity of the formulated paint, we improved and refined the classical Van der Pauw method, introducing and employing an improved Van der Pauw method based on a mixed-resistance grid. Twenty-five sample slices were utilized in the experimental design to evaluate the resistivity of the conductive paint, resulting in a resistivity of 0.001404 Ohm·m, with an accuracy percentage error of 0.65% and an uncertainty of 0.000015 Ohm·m. These experimental findings indicate that the prepared conductive paint exhibits excellent conductivity. This outstanding conductivity underscores its significant potential applications in areas such as sensors, flexible circuits, and wearable devices. Simultaneously, the experimental results demonstrate that the conductive paint we prepared maintains its conductivity stability through multiple testing sessions.

## Acknowledgments

This work was financially supported by Hangzhou Normal University Student Innovation and Entrepreneurship Fund.

## References

- [1] TRAN T S, DUTTA N K, CHOUDHURY N R. Graphene inks for printed flexible electronics: Graphene dispersions, ink formulations, printing techniques and applications [J]. *Adv Colloid Interface Sci*, 2018, 261: 41-61.
- [2] CAMARGO J R, ORZARI L O, ARAÚJO D A G, et al. Development of conductive inks for electrochemical sensors and biosensors [J]. *Microchemical Journal*, 2021, 164.
- [3] OLIVEIRA F S, CIPRIANO R B, DA SILVA F T, et al. Simple analytical method for determining electrical resistivity and sheet resistance using the van der Pauw procedure [J]. *Sci Rep*, 2020, 10(1): 16379.
- [4] ZIKULNIG J, ROSHANGHIAS A, RAUTER L, HIRSCHL C. Evaluation of the Sheet Resistance of Inkjet-Printed Ag-Layers on Flexible, Uncoated Paper Substrates Using Van-der-Pauw's Method [J]. *Sensors (Basel)*, 2020, 20(8).
- [5] PAUW L. A method of measuring specific resistivity and Hall Effect of discs of arbitrary shape [J]. *Philips Research Reports*, 1958, 13(1): 1-9.
- [6] SAHOO D, SENGUPTA P, KARAN A K, MANIK N B. Improvement in conductivity of lead-free CH<sub>3</sub>NH<sub>3</sub>SnI<sub>3</sub> perovskite thin film using multi-walled carbon nanotubes as a transporter [J]. *Surfaces and Interfaces*, 2023, 41.
- [7] GOLZ C, HORTELANO V, HATAMI F, et al. The electrical conductivity tensor of ββ-Ga<sub>2</sub>O<sub>3</sub> analyzed by van der Pauw measurements: Inherent anisotropy, off-diagonal element, and the impact of grain boundaries [J]. *Arxiv: 180608162 [physics app-ph, cond-matmtrl-sci]*, 2018.
- [8] DANNINGER S, DELFIN F A, and SCHACHINGER M, et al. Effect of deposition temperature and hydrogen as a process gas on mechanical properties and specific electrical resistivity of thick a-C: H obtained using PACVD [J]. *Surface and Coatings Technology*, 2023, 474.
- [9] HTWE Y Z N, MARIATTI M. Performance of water-based printed hybrid graphene/silver nanoparticle conductive inks for flexible strain sensor applications [J]. *Synthetic Metals*, 2023, 300.
- [10] DENNEULIN A, BLAYO A, NEUMAN C, BRAS J. Infra-red assisted sintering of inkjet printer silver tracks on paper substrates [J]. *Journal of Nanoparticle Research*, 2011, 13(9): 3815-23.
- [11] SUN Z-H, ZHOU J, XIA X-J, ZHOU D-M. Two-dimensional electrostatic model for the Van der Pauw method [J]. *Physics Letters A*, 2017, 381(27): 2144-8.
- [12] SZYMAŃSKI K R, KONDRATIUK M. Extensions of four-point methods with arbitrarily located contacts for determination of physical quantities and sheet resistance imaging [J]. *Measurement*, 2021, 178.

- [13] DERRIDA B, ZABOLITZKY J G, VANNIMENUS J, STAUFFER D. A transfer matrix program to calculate the conductivity of random resistor networks [J]. *Journal of Statistical Physics*, 1984, 36(1-2): 31-42.
- [14] HU X, ZHU L, DIAO K, et al. Electrostatic derivation for the van der Pauw formula and simulation using arbitrarily shaped resistive materials [J]. *AIP Advances*, 2022, 12(7).